



HAL
open science

Non-renormalizability of the classical statistical approximation

Thomas Epelbaum, François Gelis, Bin Wu

► **To cite this version:**

Thomas Epelbaum, François Gelis, Bin Wu. Non-renormalizability of the classical statistical approximation. *Physical Review D*, 2014, 90, pp.065029. 10.1103/PhysRevD.90.065029 . cea-01004417

HAL Id: cea-01004417

<https://cea.hal.science/cea-01004417>

Submitted on 19 Oct 2022

HAL is a multi-disciplinary open access archive for the deposit and dissemination of scientific research documents, whether they are published or not. The documents may come from teaching and research institutions in France or abroad, or from public or private research centers.

L'archive ouverte pluridisciplinaire **HAL**, est destinée au dépôt et à la diffusion de documents scientifiques de niveau recherche, publiés ou non, émanant des établissements d'enseignement et de recherche français ou étrangers, des laboratoires publics ou privés.

Nonrenormalizability of the classical statistical approximation

Thomas Epelbaum, François Gelis, and Bin Wu

*Institut de Physique Théorique (URA 2306 du CNRS),**CEA/DSM/Saclay, 91191 Gif-sur-Yvette Cedex, France*

(Received 28 April 2014; published 23 September 2014)

In this paper, we discuss questions related to the renormalizability of the classical statistical approximation, an approximation scheme that has been used recently in several studies of out-of-equilibrium problems in quantum field theory. Although the ultraviolet power counting in this approximation scheme is identical to that of the unapproximated quantum field theory, this approximation is not renormalizable. The leading cause of this nonrenormalizability is the breakdown of Weinberg's theorem in this approximation. We also discuss some practical implications of this negative result for simulations that employ this approximation scheme, and we speculate about a possible modification of the classical statistical approximation in order to systematically subtract the leading residual divergences.

DOI: 10.1103/PhysRevD.90.065029

PACS numbers: 11.10.Gh, 11.15.Kc

I. INTRODUCTION

In recent years, there has been a lot of interest in the study of out-of-equilibrium systems in quantum field theory, in view of applications to high energy heavy ion collisions, cosmology, or cold atom physics [1–33]. Generically, the question one would like to address is that of a system prepared in some nonequilibrium initial state, and allowed to evolve under the sole self-interactions of its constituents. The physically relevant quantum field theories cannot be solved exactly, and therefore some approximation scheme is mandatory in order to make progress. Moreover, the standard perturbative expansion in powers of the interaction strength is in general ill suited to these out-of-equilibrium problems. Indeed, the coefficients in the perturbative expansion are time dependent and generically growing with time, thereby voiding the validity of the expansion after some finite time.

This “secularity” problem is resolved by the resummation of an infinite set of perturbative contributions, which can be achieved via several schemes. The simplest of these schemes is kinetic theory. However, in order to obtain a Boltzmann equation from the underlying quantum field theory, several important assumptions are necessary [34]: (i) a relatively smooth system, so that a gradient expansion can be performed, and (ii) the existence of well-defined quasiparticles. These limitations, especially the latter, make kinetic theory difficult to justify for describing the early stages of heavy ion collisions.

Closer to the underlying quantum field theory, two resummation schemes have been widely considered in many works. One of them is the two-particle irreducible (2PI) approximation [28,35–46]. This scheme consists in solving the Dyson-Schwinger equations for the two-point functions (and possibly for the expectation value of the field, if it differs from zero). The self-energy diagrams that are resummed on the propagator are obtained

self-consistently from the sum of 2PI skeleton vacuum diagrams (often denoted $\Gamma_2[G]$ in the literature). The only approximation arises from the practical necessity of truncating the functional $\Gamma_2[G]$ in order to have manageable expressions. In applications, the 2PI scheme suffers from two limitations. One of them is purely computational: the convolution of the self-energy with the propagator takes the form of a memory integral, that in principle requires that one stores the entire history of the evolution of the system, from the initial time to the current time. The needed storage therefore grows quadratically with time.¹ The second difficulty appears in systems that are the siege of large fields, or large occupation numbers. For instance, in QCD, “large” would mean of order g^{-1} for the fields, and of order g^{-2} for the gluon occupation number. In this regime, the functional $\Gamma_2[G]$ contains terms that have the same order of magnitude at every order in the loop expansion, and therefore one cannot justify truncating it at a finite loop order.² It turns out that these problems of strong fields occur in real world problems, e.g. in the early stages of heavy ion collisions [47–51].

There is an alternative resummation scheme, that includes all the leading contributions in the large field regime and is similarly free of secular terms, called the classical statistical approximation (CSA) [52–57]. It owes its name to the way it is implemented in practice, as an average over classical solutions of the field equations of motion, with a Gaussian statistical ensemble of initial

¹This can be alleviated somewhat by an extra approximation, in which one stores only the “recent” history of the system, in a sliding time window that moves with the current time.

²Such a truncation becomes legitimate, even in the large field regime, if there is an additional expansion parameter that one can use to control the loop expansion in $\Gamma_2[G]$. In some theories with a large number N of constituents [e.g. an $O(N)$ scalar theory in the limit $N \rightarrow \infty$], one can compute exactly the leading term of $\Gamma_2[G]$ in the $1/N$ expansion [40].

conditions. The ability of this method to remain valid in the large field regime comes with a tradeoff: the CSA can be tuned to be exact at the one-loop level, but starting at the two-loop order and beyond, it includes only a subset of all the possible contributions. The CSA can be derived via several methods: from the path integral representation of observables [57], as an approximation at the level of the diagrammatic rules in the retarded-advanced formalism, or as an exponentiation of the one-loop result [55].

The diagrammatic rules that define the classical statistical approximation allow graphs that have arbitrarily many loops. As in any field theory, the loops that arise in this expansion involve an integral over a 4-momentum, and this integral can be ultraviolet divergent. In the underlying—non approximated—field theory, we know how to deal with these infinities by redefining a finite number of parameters of the Lagrangian (namely the coupling constant, the mass and the field normalization). In general, this is done by first introducing an ultraviolet regulator, for instance a momentum cutoff Λ_{UV} on the loop momenta, and by letting the bare parameters of the Lagrangian depend on Λ_{UV} in such a way that physical quantities are independent of Λ_{UV} (and of course are finite in the limit $\Lambda_{UV} \rightarrow \infty$). That this redefinition is possible is what characterizes a renormalizable field theory.

In contrast, nonrenormalizable theories are theories in which one needs to introduce new operators that did not exist in the Lagrangian one started from, in order to subtract all the ultraviolet divergences that arise in the loop expansion. This procedure defines an “ultraviolet completion” of the original theory, which is well defined at arbitrary energy scales. The predictive power of the original theory is limited by the order at which it becomes necessary to introduce these new operators.³

It can also happen that, starting from a renormalizable field theory, certain approximations of this theory (for instance including certain loop corrections, but not all of them) are not renormalizable. This will be our main concern in this paper, in the context of the classical statistical approximation. A recent numerical study [5] showed a pronounced cutoff dependence for rather large couplings in a computation performed in this approximation scheme. This could either mean that the CSA is not renormalizable, or that the CSA is renormalizable but that renormalization was not performed properly in this computation. It is therefore of utmost importance to determine to which class—renormalizable or nonrenormalizable—the CSA belongs, since this has far-reaching practical implications on how it can be used in order to make predictive calculations, and how to interpret the existing computations.

³The predictive power of its ultraviolet completion may be quite limited as well, depending on how many new operators need to be introduced at each order (especially if this number grows very quickly or even worse becomes infinite).

Note that the question of the renormalizability of classical approximation schemes has already been discussed in quantum field theory at finite temperature [58–62], following attempts to calculate nonperturbatively the sphaleron transition rate [63–70]. In this context, one is calculating the leading high temperature contribution, and in the classical approximation the Bose-Einstein distribution gets replaced by T/ω_k . This approximation leads to ultraviolet divergences in thermal contributions, that would otherwise be finite thanks to the exponential tail of the Bose-Einstein distribution. However, it has been shown that only a finite number of graphs has such divergences, and that they can all be removed by appropriate counterterms. The problem we will consider in this paper is different since we are interested in the classical approximation of a zero-temperature quantum field theory, where the factors T/ω_k are replaced by $1/2$. This changes drastically the ultraviolet behavior.

In Sec. II, we expose the scalar toy model we are going to use throughout the paper as support for this discussion, we also remind the reader of the closed time path formalism and of the retarded-advanced formalism (obtained from the latter via a simple field redefinition), and we present the classical statistical approximation in two different ways (one that highlights its diagrammatic rules, and one that is more closely related to the way it is implemented in numerical simulations). Then, we analyze in Sec. III the ultraviolet power counting in the CSA, and show that it is identical to that in the underlying field theory. In Sec. IV, we examine all the one-loop two-point and four-point functions in the CSA, and we show that one of them violates Weinberg’s theorem. This leads to contributions that are nonrenormalizable in the CSA. In Sec. V, we discuss the implications of nonrenormalizability of the CSA for the calculation of some observables. We also argue that it may be possible to systematically subtract the leading nonrenormalizable terms by the addition of a complex noise term to the classical equations of motion. Finally, Sec. VI is devoted to concluding remarks. Some technical derivations are relegated into two appendixes.

II. PRELIMINARIES

A. Toy model

In order to illustrate our point, let us consider a massless real scalar field ϕ in four space-time dimensions, with quartic self-coupling, and coupled to an external source $j(x)$ (therefore mimicking the color glass condensate framework used in the context of heavy ion collisions),

$$\mathcal{L} \equiv \frac{1}{2}(\partial_\mu \phi)(\partial^\mu \phi) - \frac{m^2}{2}\phi^2 - \frac{g^2}{4!}\phi^4 + j\phi. \quad (1)$$

In this model, $j(x)$ is a real valued function, given once for all as a part of the description of the model. Sufficient regularity and compactness of this function will be assumed as necessary.

We also assume that the state of the system at $x^0 = -\infty$ is the vacuum state (by adiabatically turning off the couplings at asymptotic times, we can assume that this is the perturbative vacuum state $|0_{\text{in}}\rangle$). Because of the coupling to the external source $j(x)$, the system is driven away from the vacuum state, and observables measured at later times acquire nontrivial values. Our goal is to compute the expectation value of such observables, expressed in terms of the field operator and its derivatives, in the course of the evolution of the system,

$$\langle \mathcal{O} \rangle \equiv \langle 0_{\text{in}} | \mathcal{O}[\phi, \partial\phi] | 0_{\text{in}} \rangle. \quad (2)$$

For simplicity, one may assume that the observable is a local (i.e. depends on the field operator at a single space-time point) or multilocal operator (i.e. depends on the field operator at a finite set of space-time points).

B. Closed time path formalism

It is well known that the proper framework to compute expectation values such as the one defined in Eq. (2) is the Schwinger-Keldysh (or “closed time path”) formalism [71,72]. In this formalism, there are two copies ϕ_+ and ϕ_- of the field (corresponding respectively to fields in amplitudes and fields in complex conjugated amplitudes), and four bare propagators depending on which type of fields they connect. The expectation value of Eq. (2) can be expanded diagrammatically (each loop brings an extra power of the coupling g^2) by a set of rules that generalizes the traditional Feynman rules in a simple manner:

- (i) Each vertex of a graph can be of type $+$ or $-$, and for a given graph topology one must sum over all the possible assignments of the types of these vertices. The rules for the $+$ vertex ($-ig^2$) and for the $-$ vertex ($+ig^2$) differ only in their sign. The same rule applies to the external source j .
- (ii) A vertex of type ϵ and a vertex of type ϵ' must be connected by a bare propagator $G_{\epsilon\epsilon'}^0$. In momentum space, these bare propagators read

$$\begin{aligned} G_{++}^0(p) &= \frac{i}{p^2 - m^2 + i\epsilon}, \\ G_{--}^0(p) &= \frac{-i}{p^2 - m^2 - i\epsilon}, \\ G_{+-}^0(p) &= 2\pi\theta(-p^0)\delta(p^2 - m^2), \\ G_{-+}^0(p) &= 2\pi\theta(p^0)\delta(p^2 - m^2). \end{aligned} \quad (3)$$

Note that since the initial state in the observable (2) is the $|0_{\text{in}}\rangle$ vacuum state, the G_{++}^0 and G_{--}^0 propagators are vacuum propagators [contrary to quantum field theory at finite temperature, where they would contain an additional term that depends on the distribution $f(\mathbf{p})$ of particles in the thermal bath]. The four bare propagators of the Schwinger-Keldysh formalism are related by a simple algebraic identity,

$$G_{++}^0 + G_{--}^0 = G_{+-}^0 + G_{-+}^0, \quad (4)$$

that one can check immediately from Eqs. (3). Note that, on a more fundamental level, this identity follows from the definition of the various $G_{\epsilon\epsilon'}$ as vacuum expectation values of pairs of fields ordered in various ways. For this reason, it is true not only for the bare propagators, but for their corrections at any order in g^2 .

C. Retarded-advanced formalism

The Schwinger-Keldysh formalism is not the only one that can be used to calculate Eq. (2). One can arrange the four bare propagators $G_{\epsilon\epsilon'}^0$ in a 2×2 matrix, and obtain equivalent diagrammatic rules by applying a “rotation” to this matrix [61,73–75]. Among this family of transformations, especially interesting are those that exploit the linear relationship (4) among the $G_{\epsilon\epsilon'}^0$ in order to obtain a vanishing entry in the rotated matrix. The retarded-advanced formalism belongs to this class of transformations, and its propagators are defined by (let us denote $\alpha = 1, 2$ the two values taken by the new index)

$$\mathbb{G}_{\alpha\beta}^0 \equiv \sum_{\epsilon, \epsilon' = \pm} \Omega_{\alpha\epsilon} \Omega_{\beta\epsilon'} G_{\epsilon\epsilon'}^0, \quad (5)$$

with the transformation matrix is defined as

$$\Omega_{\alpha\epsilon} \equiv \begin{pmatrix} 1 & -1 \\ 1/2 & 1/2 \end{pmatrix}. \quad (6)$$

The bare rotated propagators read

$$\mathbb{G}_{\alpha\beta}^0 = \begin{pmatrix} 0 & G_A^0 \\ G_R^0 & G_S^0 \end{pmatrix}, \quad (7)$$

where we have introduced

$$\begin{aligned} G_R^0 &= G_{++}^0 - G_{+-}^0, & G_A^0 &= G_{++}^0 - G_{-+}^0, \\ G_S^0 &= \frac{1}{2}(G_{++}^0 + G_{--}^0). \end{aligned} \quad (8)$$

(The subscripts R , A and S stand respectively for “retarded,” “advanced” and “symmetric.”) Again, because the initial state in Eq. (2) is the vacuum, the propagator G_S^0 is a pure vacuum propagator:

$$G_S^0(p) = \pi\delta(p^2 - m^2). \quad (9)$$

It is straightforward to verify that in the rotated formalism, the various vertices read

$$\Gamma_{\alpha\beta\gamma\delta} \equiv -ig^2 [\Omega_{+\alpha}^{-1} \Omega_{+\beta}^{-1} \Omega_{+\gamma}^{-1} \Omega_{+\delta}^{-1} - \Omega_{-\alpha}^{-1} \Omega_{-\beta}^{-1} \Omega_{-\gamma}^{-1} \Omega_{-\delta}^{-1}], \quad (10)$$

where

$$\Omega_{\epsilon\alpha}^{-1} = \begin{pmatrix} 1/2 & 1 \\ -1/2 & 1 \end{pmatrix} [\Omega_{\alpha\epsilon} \Omega_{\epsilon\beta}^{-1} = \delta_{\alpha\beta}]. \quad (11)$$

More explicitly, we have

$$\begin{aligned} \Gamma_{1111} &= \Gamma_{1122} = \Gamma_{2222} = 0 \\ \Gamma_{1222} &= -ig^2, \quad \Gamma_{1112} = -ig^2/4. \end{aligned} \quad (12)$$

(The vertices not listed explicitly here are obtained by trivial permutations.) Concerning the insertions of the external source, the diagrammatic rules in the retarded-advanced formalism are

$$J_1 = ij, \quad J_2 = 0. \quad (13)$$

D. Trading the source j for an external classical field

From the above rules, we see that an external source can only be attached to a propagator end point of type 1, i.e. to the lowest time end point of a retarded or advanced propagator ($G_{12}^0 = G_A^0$, $G_{21}^0 = G_R^0$), as in the formula

$$\int d^4y G_{21}^0(x, y) J_1(y). \quad (14)$$

(This expression corresponds to the first graph on the left of Fig. 1.) It is easy to see that the external source can be summed to all orders, if one introduces the object $\varphi(x)$ defined diagrammatically in Fig. 1. It is well known that this series obeys the classical equation of motion,

$$(\square + m^2)\varphi + \frac{g^2}{6}\varphi^3 = j, \quad (15)$$

and since all the propagators are all of type G_{21}^0 , i.e. retarded, it obeys the following boundary condition:

$$\lim_{x^0 \rightarrow -\infty} \varphi(x) = 0. \quad (16)$$

The source j can be completely eliminated from the diagrammatic rules, by adding to the Lagrangian couplings between the field operator ϕ and the classical field φ ,

$$\Delta\mathcal{L} \equiv g^2 \left[\frac{1}{2} \varphi^2 \phi_1 \phi_2 + \frac{1}{2} \varphi \phi_1 \phi_2^2 + \frac{1}{4!} \varphi \phi_1^3 \right]. \quad (17)$$

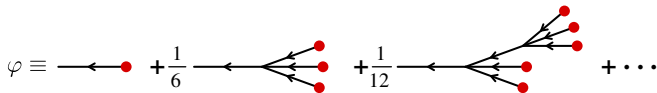


FIG. 1 (color online). The first three terms of the diagrammatic expansion of the external field in terms of the external source, for a field theory with quartic coupling. The red dots represent the source insertions J_1 , and the lines with an arrow are bare retarded propagators G_{21}^0 . The quartic vertices are all of the type Γ_{1222} .

Note that, since in all the graphs in Fig. 1 the root of the tree is terminated by an index 2, the classical field φ can only be attached to an index of type 2 in these vertices.

E. Classical statistical approximation (CSA)

1. Definition as truncated retarded-advanced rules

The classical statistical approximation consists in dropping all the graphs that contain the vertex Γ_{2111} , under the assumption that $\phi_1 \ll \phi_2$, φ , i.e. in assuming

$$\Gamma_{2111} = 0 \quad (\text{and similarly for the permutations of } 2111). \quad (18)$$

In the rest of this paper, we will simply call CSA the field theory obtained by dropping all the vertices that have 3 indices of type 1 in the retarded-advanced formalism, while everything else remains unchanged. Therefore, in the retarded-advanced formalism, the CSA is defined by the following diagrammatic rules:

(i) *bare propagators:*

$$\begin{aligned} G_{21}^0(p) &= \frac{i}{(p^0 + i\epsilon)^2 - \mathbf{p}^2 - m^2}, \\ G_{12}^0(p) &= \frac{i}{(p^0 - i\epsilon)^2 - \mathbf{p}^2 - m^2}, \\ G_{22}^0(p) &= \pi\delta(p^2 - m^2). \end{aligned} \quad (19)$$

(ii) *vertices:*

$$\begin{aligned} \Gamma_{1222} \quad (\text{and permutations}) &= -ig^2, \\ \text{all other combinations} &= 0. \end{aligned} \quad (20)$$

(iii) *external sources:*

$$J_1 = ij, \quad J_2 = 0. \quad (21)$$

(iii') *external field (see Sec. II D):*

$$\Phi_1 = 0, \quad \Phi_2 = \varphi. \quad (22)$$

Note that this “truncated” field theory is still quite nontrivial, in the sense that the above diagrammatic rules allow graphs with arbitrarily many loops. In fact, all the topologies that exist in the full theory also exist in the CSA, but with some restrictions regarding the possible assignments of 1 and 2 indices. The numerical simulations that implement the CSA provide the sum to all orders of the graphs that can be constructed with these rules (with an accuracy in principle only limited by the statistical errors in the Gaussian average

over the initial field fluctuations, since this average is approximated by a Monte Carlo sampling).

2. Definition by exponentiation of the one-loop result

The previous definition of the CSA makes it very clear what graphs are included in this approximation and what graphs are not. However, it is a bit remote from the actual numerical implementation. Let us also present here an alternative—but strictly equivalent—way of introducing the classical statistical approximation, that directly provides a formulation that can be implemented numerically.

Firstly, observables at leading order⁴ (tree level) are expressible in terms of the retarded classical field φ introduced above [76],

$$\langle 0_{\text{in}} | \mathcal{O}[\phi, \partial\phi] | 0_{\text{in}} \rangle_{\text{LO}} = \mathcal{O}[\varphi, \partial\varphi]. \quad (23)$$

At next-to-leading order (one loop), it has been shown in [55,77,78] that the observable (2) can be expressed as follows:

$$\begin{aligned} \langle 0_{\text{in}} | \mathcal{O}[\phi, \partial\phi] | 0_{\text{in}} \rangle_{\text{NLO}} \\ = \left[\frac{1}{2} \int \frac{d^3\mathbf{k}}{(2\pi)^3 2E_{\mathbf{k}}} \int d^3\mathbf{u} d^3\mathbf{v} (\boldsymbol{\alpha}_{\mathbf{k}} \cdot \mathbb{T}_{\mathbf{u}}) (\boldsymbol{\alpha}_{\mathbf{k}}^* \cdot \mathbb{T}_{\mathbf{v}}) \right] \\ \times \mathcal{O}[\varphi, \partial\varphi]. \end{aligned} \quad (24)$$

In Eq. (24), the operator $\mathbb{T}_{\mathbf{u}}$ is the generator of shifts of the initial condition for the classical field φ on some constant time surface (the integration surface for the variables \mathbf{u} and \mathbf{v}) located somewhere before the source j is turned on.⁵ This means that if we denote $\varphi[\varphi_{\text{init}}]$ the classical field as a functional of its initial condition, then for any functional $F[\varphi]$ of φ , we have

$$\left[\exp \int d^3\mathbf{u} (a \cdot \mathbb{T}_{\mathbf{u}}) \right] F[\varphi[\varphi_{\text{init}}]] = F[\varphi[\varphi_{\text{init}} + a]]. \quad (25)$$

(This equation can be taken as the definition of $\mathbb{T}_{\mathbf{u}}$.) In Eq. (24), the fields $\boldsymbol{\alpha}_{\mathbf{k}}$ are free plane waves of momentum k^μ ($k^2 = m^2$):

$$\boldsymbol{\alpha}_{\mathbf{k}}(u) \equiv e^{ik \cdot u}, \quad (\square + m^2)\boldsymbol{\alpha}_{\mathbf{k}}(u) = 0. \quad (26)$$

Note that in Eq. (24), the integration variable \mathbf{k} is a loop momentum. In general, the integral over \mathbf{k} therefore diverges in the ultraviolet, and must be regularized by a

⁴Note that in the presence of a strong external $j \sim g^{-1}$, the leading order is the sum of an infinite set of tree level graphs. Similarly, the next-to-leading order comprises an infinite number of one-loop graphs. The formulas (23) and (24) do include these complete sets of graphs, respectively at LO and NLO.

⁵This is why Eq. (24) does not have a term linear in $\mathbb{T}_{\mathbf{u}}$, contrary to the slightly more general formulas derived in Refs. [55,77,78].

cutoff. In a renormalizable theory, after the Lagrangian parameters have been renormalized at one loop, this cutoff can be safely sent to infinity.⁶

In this framework, the classical statistical method is defined as the result of the exponentiation of the operator that appears in the right-hand side of Eq. (24),

$$\begin{aligned} \langle 0_{\text{in}} | \mathcal{O}[\phi, \partial\phi] | 0_{\text{in}} \rangle_{\text{CSA}} \\ = \exp \left[\frac{1}{2} \int \frac{d^3\mathbf{k}}{(2\pi)^3 2E_{\mathbf{k}}} \int d^3\mathbf{u} d^3\mathbf{v} (\boldsymbol{\alpha}_{\mathbf{k}} \cdot \mathbb{T}_{\mathbf{u}}) (\boldsymbol{\alpha}_{\mathbf{k}}^* \cdot \mathbb{T}_{\mathbf{v}}) \right] \\ \times \mathcal{O}[\varphi, \partial\varphi]. \end{aligned} \quad (27)$$

Note that by construction, the CSA is identical to the underlying theory at leading order (LO) and next-to-leading order (NLO), and starts differing from it at next-to-next-to-leading order (NNLO) and beyond (some higher loop graphs are included but not all of them). The relation between this formula and the way the classical statistical method is implemented lies in the fact that the exponential operator is equivalent to a Gaussian average over a Gaussian distribution of initial conditions for the classical field φ ,

$$\begin{aligned} \exp \left[\frac{1}{2} \int \frac{d^3\mathbf{k}}{(2\pi)^3 2E_{\mathbf{k}}} \int d^3\mathbf{u} d^3\mathbf{v} (\boldsymbol{\alpha}_{\mathbf{k}} \cdot \mathbb{T}_{\mathbf{u}}) (\boldsymbol{\alpha}_{\mathbf{k}}^* \cdot \mathbb{T}_{\mathbf{v}}) \right] F[\varphi[\varphi_{\text{init}}]] \\ = \int [Da(\mathbf{u}) D\dot{a}(\mathbf{u})] G[a, \dot{a}] F[\varphi[\varphi_{\text{init}} + a]], \end{aligned} \quad (28)$$

where $G[a, \dot{a}]$ is a Gaussian distribution, whose elements can be generated as

$$a(u) = \int \frac{d^3\mathbf{k}}{(2\pi)^3 2E_{\mathbf{k}}} [c_{\mathbf{k}} \boldsymbol{\alpha}_{\mathbf{k}}(u) + c_{\mathbf{k}}^* \boldsymbol{\alpha}_{\mathbf{k}}^*(u)], \quad (29)$$

with $c_{\mathbf{k}}$ complex Gaussian random numbers defined by

$$\langle c_{\mathbf{k}} \rangle = 0, \quad \langle c_{\mathbf{k}} c_{\mathbf{l}} \rangle = 0, \quad \langle c_{\mathbf{k}} c_{\mathbf{l}}^* \rangle = (2\pi)^3 E_{\mathbf{k}} \delta(\mathbf{k} - \mathbf{l}). \quad (30)$$

In some works, a variant of these initial conditions has been considered:

$$\langle c_{\mathbf{k}} c_{\mathbf{l}}^* \rangle = (2\pi)^3 E_{\mathbf{k}} (2f(\mathbf{k})) \delta(\mathbf{k} - \mathbf{l}), \quad (31)$$

where $f(\mathbf{k})$ is an initial distribution of quasiparticles. In this setup, the fluctuations are due to initial particle excitations instead of vacuum fluctuations [both types of fluctuations can be included at the same time by the replacement $2f(\mathbf{k}) \rightarrow 1 + 2f(\mathbf{k})$]. The renormalizability of the CSA has already been studied with initial fluctuations of type (31) in Refs. [58–62] when $f(\mathbf{k}) \sim 1/|\mathbf{k}|$, i.e. for a system prepared in a classical thermal equilibrium state. In this case, it was found that the CSA is super-renormalizable; i.e. it can

⁶In the case of composite operators such as the energy-momentum tensor, additional subtractions may be required.

be renormalized with a finite number of subtractions [it would be totally UV finite if $f(\mathbf{k})$ falls faster than $1/|\mathbf{k}|$]. Situations where the initial state can be described by Eq. (31) are thus not problematic from the point of view of UV divergences (in this case, the validity of the CSA amounts to the condition $f(\mathbf{k}) \gg 1$ [79]). However, the color glass condensate-like setup that we have chosen in Eqs. (1) and (2) does not lead to this type of initial conditions, but to Eq. (30). In the rest of this paper, we consider only vacuum fluctuations, given in Eq. (30).

We will not reproduce here the proof of the equivalence among Eqs. (28), (29), (30) and the classical statistical approximation as introduced in Sec. II E 1. The main reason for recalling the second definition of the CSA was to emphasize the origin of the variable \mathbf{k} in Eqs. (24), (27) and (29), as a loop momentum. Therefore, an upper limit introduced in the \mathbf{k} integration in any of these formulas will effectively play the role of an ultraviolet cutoff that regularizes loop integrals.

To make the connection with the diagrammatic rules of the classical statistical approximation introduced in the previous subsection, the cutoff on the momentum of the initial fluctuations is equivalent to an upper limit for the momentum flowing through the G_{22}^0 propagators. In contrast, the largest momentum that can flow through the G_{21}^0 and G_{12}^0 propagators is only controlled by the discretization of space, i.e. by the inverse lattice spacing. In some implementations, these two cutoffs are identical, but other implementations have chosen to restrict the possible momenta of the initial fluctuations:

- (i) In Refs. [2–4,80] an explicit cutoff Λ_{UV} , distinct from the lattice cutoff, is introduced in order to limit the largest \mathbf{k} of the initial fluctuations. In Refs. [81–83], fluctuations are only included for modes that may be subject to some instability. In these setups, Λ_{UV} is smaller than the lattice momentum cutoff, and the lattice spacing no longer controls the ultraviolet limit of the computation.
- (ii) In Refs. [5,13–15,17] fluctuation modes are included up to the lattice momentum cutoff; i.e. Λ_{UV} is inversely proportional to the lattice spacing.

A common caveat of most of these computations is that none has studied the behavior of the results in the limit $\Lambda_{\text{UV}} \rightarrow \infty$, with the exception of Ref. [5] where a strong dependence on the ultraviolet cutoff was observed.

III. ULTRAVIOLET POWER COUNTING

After having defined the classical statistical approximation, we can first calculate the superficial degree of ultraviolet divergence for arbitrary graphs in the CSA, in order to see what kind of divergences one may expect. This is best done by using the definition introduced in Sec. II E 1, that defines the CSA by its diagrammatic rules.

Let us consider a generic *connected* graph \mathcal{G} built with these diagrammatic rules, made of

- (i) E external legs
- (ii) I internal lines
- (iii) L independent loops
- (iv) V vertices of type ϕ^4
- (v) V_2 vertices of type $\phi^2\phi^2$
- (vi) V_1 vertices of type $\phi^3\phi$

Note that for the internal lines, the superficial degree of divergence does not distinguish⁷ among the propagators G_{12}^0 , G_{21}^0 and G_{22}^0 , because they all have a mass dimension -2 . These numbers are related by the following relations:

$$E + 2I = 4V + 3V_1 + 2V_2, \quad (32)$$

$$L = I - (V + V_1 + V_2) + 1. \quad (33)$$

The first of these identities states that the number of propagator end points must be equal to the number of slots where they can be attached to vertices. The second identity counts the number of independent momenta that can circulate in the loops of the graph.

In terms of these quantities, the superficial degree of divergence of the graph \mathcal{G} is given by

$$\begin{aligned} \omega(\mathcal{G}) &= 4L - 2I \\ &= 4 - E - (V_1 + 2V_2) \\ &= 4 - E - N_\varphi, \end{aligned} \quad (34)$$

where $N_\varphi \equiv V_1 + 2V_2$ is the number of powers of the external classical field φ inserted into the graph \mathcal{G} .

Note that $4 - E$ is the superficial degree of divergence of a graph with E external points in a four-dimensional scalar ϕ^4 theory, in the absence of an external field/source. Therefore, the external field can only decrease the superficial degree of divergence (since $N_\varphi \geq 0$), which was expected since the couplings to the external field [see Eq. (17)] have a positive mass dimension; i.e. they are super-renormalizable interactions.

The crucial point about this formula is that the superficial degree of divergence does not depend on the fact that we have excluded the vertices of type 2111 in the classical statistical approximation. In other words, the ultraviolet power counting is exactly the same in the full theory and in the CSA. Equation (34) suggests that the only ultraviolet divergent quantities are those for which $E \leq 4$, exactly as in the unapproximated theory.

As we shall see in the next section, there is nevertheless an issue that hinders the renormalizability of the classical statistical approximation. Discarding the Γ_{1112} alters in subtle ways the analytic structure of Green's functions, which leads to a violation of Weinberg's

⁷As we shall see later, due to the peculiar analytic structure of the integrands of graphs in the CSA, this power counting is too naive to accurately reflect the actual ultraviolet divergences.

theorem.⁸ As a consequence, ultraviolet divergences in the CSA can be stronger than one would expect on the basis of the power counting alone.

IV. ULTRAVIOLET DIVERGENCES IN THE CSA

A. Introduction

The untruncated ϕ^4 theory that we started from is well known to be renormalizable.⁹ This means that all its ultraviolet divergences can be disposed of by redefining the coefficients in front of the operators that appear in the bare Lagrangian.

In the retarded-advanced basis, the Lagrangian of the CSA differs from the Lagrangian of the unapproximated theory in the fact that the vertex Γ_{1112} is missing. All the other terms of the Lagrangian are unchanged, in particular the operators that are quadratic in the fields. In this section we systematically examine two- and four-point functions at one loop, in order to see whether their ultraviolet behavior is compatible with renormalizability or not.

If one assumes that $j \sim \frac{1}{g}$ (or, equivalently, $\varphi \sim \frac{1}{g}$), the propagators dressed by the background field φ are of the same order as the bare ones. In addition, some field modes that were initially small may grow exponentially at the initial time in systems with instabilities. In these cases, a consistent calculation requires the resummation of an infinite number of diagrams. However, the dressing of a propagator by an external field does not change its behavior in the ultraviolet [Eq. (34) shows that external field insertions lower the degree of UV divergence]. Therefore the discussion of renormalizability can be done in terms of the bare propagators listed in Eqs. (19).

B. Self-energies at one loop

Let us start with the simplest possible loop correction: the one-loop self-energy, made of a tadpole graph. Depending on the indices 1 and 2 assigned to the two external legs, these self-energies are given in Eq. (35):

$$\begin{aligned}
 -i[\Sigma_{11}]_{\text{CSA}}^{1 \text{ loop}} &= 0, & -i[\Sigma_{22}]_{\text{CSA}}^{1 \text{ loop}} &= \frac{\text{tadpole}(2,1)}{2 \cdot 2} = 0 \\
 -i[\Sigma_{12}]_{\text{CSA}}^{1 \text{ loop}} &= \frac{\text{tadpole}(2,2)}{1 \cdot 2} = -i \frac{g^2 \Lambda_{\text{UV}}^2}{16\pi^2}.
 \end{aligned} \tag{35}$$

Σ_{11} is zero at one loop in the CSA, because it requires a vertex 1112 that has been discarded. Σ_{22} is also zero, because it contains a closed loop made of a retarded propagator. The only nonzero self-energy at one loop is Σ_{12} , that displays the usual quadratic divergence. This can be removed by a mass counterterm in the Lagrangian,

$$\delta m^2 = -\frac{g^2 \Lambda_{\text{UV}}^2}{16\pi^2}, \tag{36}$$

since the mass term in the Lagrangian is precisely a $\phi_1 \phi_2$ operator.

⁸In addition to power counting arguments, renormalizability requires some handle on the recursive structure of the ultraviolet divergences. This may come in the form of Dyson's convergence theorem [84], whose proof was completed by Weinberg [85] and somewhat simplified by Hahn and Zimmermann [86,87] (see also Refs. [88,89]). This result states that if all the divergences in the subgraphs of a given graph \mathcal{G} have been subtracted, then the remaining divergence is a polynomial of degree $\omega(\mathcal{G})$ in the external momenta.

⁹The fact that we are dealing here with a field theory coupled to an external source does not spoil this property, for sufficiently smooth external sources. See Ref. [90], Chapter 11.

C. Four-point functions at one loop

1. Vanishing functions: Γ_{1112} , Γ_{1111} and Γ_{2222}

The four-point function with indices 1112 is a prime suspect for Green's functions that may cause problems with the renormalizability of the CSA. Indeed, the CSA consists in discarding the operator corresponding to this vertex from the Lagrangian. Therefore, if an intrinsic¹⁰ ultraviolet divergent contribution to this Green's function can be generated in the classical statistical approximation, then the CSA is not renormalizable.

Let us first consider this four-point function at one loop. At this order, the only possible contribution (up to trivial permutations of the external legs) to the Γ_{1112} function is

$$-i\Gamma_{1112}^{1 \text{ loop}} = \frac{\text{bubble}(1,1,2,2)}{1 \cdot 2 \cdot 2 \cdot 2}, \tag{37}$$

¹⁰Here, we are talking about the overall divergence of the function, not the divergences associated to its various subgraphs, that may be subtracted by having renormalized the other operators of the Lagrangian.

where the indices 1 and 2 indicate the various vertex assignments. (The $-i$ prefactor is a convention, so that the function Γ can be viewed directly as a correction to the coupling constant g^2 .) Because it must contain a vertex of type 112, this function is zero in the classical statistical approximation,¹¹

$$-i[\Gamma_{1112}]_{\text{CSA}}^{1\text{ loop}} = 0. \quad (38)$$

Therefore, this four-point function does not cause any renormalization problem in the CSA at one loop. Similarly, the function Γ_{1111} at one loop also requires the vertex 112, and is therefore zero in the classical statistical approximation,¹²

$$-i[\Gamma_{1111}]_{\text{CSA}}^{1\text{ loop}} = 0. \quad (39)$$

For the function Γ_{2222} at one loop, the only possibility is the following:

$$-i[\Gamma_{2222}]_{\text{CSA}}^{1\text{ loop}} = \text{Diagram} = 0, \quad (40)$$

where we have represented with arrows the 12 propagators, since they are retarded propagators. This graph is zero because it is made of a sequence of retarded propagators forming a closed loop.

2. Logarithmic divergence in Γ_{1222}

At one loop, the function Γ_{1222} is given by the graph of Eq. (41) (and several other permutations of the indices):

$$-i[\Gamma_{1222}]_{\text{CSA}}^{1\text{ loop}} = \text{Diagram} \sim g^4 \log(\Lambda_{\text{UV}}). \quad (41)$$

It is a straightforward calculation to check that this graph has a logarithmic ultraviolet divergence, that can be removed by the standard one-loop renormalization of the coupling constant (this is possible, since the interaction term $\phi_1\phi_2^3$ has been kept in the Lagrangian when doing the classical statistical approximation). The calculation of this four-point function is detailed in Appendix A.

3. Violation of Weinberg's theorem in Γ_{1122}

Another interesting object to study is the four-point function with indices 1122. There is no such bare vertex in the Lagrangian (both for the unapproximated theory and for the classical statistical approximation). Since the full theory is renormalizable, this function should not have ultraviolet divergences at one loop, since such divergences would not be renormalizable. However, since the CSA discards certain terms, it is not obvious *a priori* that this conclusion still holds. For the sake of definiteness, let us denote p_1, \dots, p_4 the external momenta of this function (defined to be all incoming into the graph, and therefore $p_1 + p_2 + p_3 + p_4 = 0$), and let us assume that the two indices 1 are attached to the legs p_1, p_2 and the two indices 2 are attached to the legs p_3, p_4 . At one loop, this four-point function (in the full field theory) receives the following contributions:

$$-i\Gamma_{1122}^{1\text{ loop}} = \text{S channel} + \text{T channel} + \text{U channel} \quad (42)$$

¹¹For the calculation of the full Γ_{1112} at one loop, beyond the classical statistical approximation, see Appendix A.

¹²At one loop, the functions Γ_{1111} and Γ_{2222} are also zero in the full theory.

Since the full theory is renormalizable, the sum of all these graphs should be ultraviolet finite, because there is no 1122 four-field operator in the bare Lagrangian.

It is however not obvious that the subset of these graphs that exists in the classical statistical approximation is itself ultraviolet finite. Among the T-channel and U-channel graphs, only the first of the three graphs exist in the CSA, since all the other graphs contain the 1112 bare vertex,

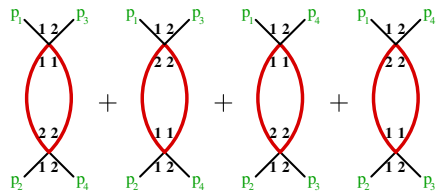
$$-i[\Gamma_{1122}]_{\text{CSA}}^{1\text{ loop}} = \begin{array}{c} p_1 \quad p_3 \\ \diagdown \quad / \\ \text{2 2} \\ / \quad \diagdown \\ p_2 \quad p_4 \end{array} + \begin{array}{c} p_1 \quad p_4 \\ \diagdown \quad / \\ \text{2 2} \\ / \quad \diagdown \\ p_2 \quad p_3 \end{array}. \quad (43)$$

Some details of the calculation of these graphs are provided in Appendix B. One obtains

$$-i[\Gamma_{1122}]_{\text{CSA}}^{1\text{ loop}} = -\frac{g^4}{64\pi} \left[\text{sign}(T) + \text{sign}(U) + 2\Lambda_{\text{UV}} \left(\frac{\theta(-T)}{|\mathbf{p}_1 + \mathbf{p}_3|} + \frac{\theta(-U)}{|\mathbf{p}_1 + \mathbf{p}_4|} \right) \right], \quad (44)$$

where we denote

$$T \equiv (p_1 + p_3)^2, \quad U \equiv (p_1 + p_4)^2, \quad (45)$$



and where Λ_{UV} is an ultraviolet cutoff introduced to regularize the integral over the 3-momentum running in the loop. As one sees, these graphs have a *linear* ultraviolet divergence, despite having a superficial degree of divergence equal to zero. This property violates Weinberg's theorem since, if it were applicable here, it would imply at most a logarithmic divergence with a coefficient independent of the external momenta. One can attribute this violation to the analytic structure of the integrand¹³: unlike in ordinary Feynman perturbation theory, we cannot perform a Wick rotation to convert the integral to an integral over an Euclidean momentum, which is an important step in the proof of Weinberg's theorem.

Since it occurs in the operator $\phi_1^2 \phi_2^2$, which does not appear in the CSA Lagrangian, this linear divergence provides incontrovertible proof of the fact that *the classical statistical approximation is not renormalizable*. Moreover, this conclusion is independent of the value of the coupling constant. The only thing one gains at smaller coupling is that the irreducible cutoff dependence caused by these terms is weaker.

It should also be noted that this linear divergence is a purely imaginary contribution to the function Γ_{1122} (this can be understood from the structure of the integrand, that was made of two delta functions, which is reminiscent of the calculation of the imaginary part of a Green's function via Cutkosky's cutting rules [91,92]).

In Appendix B, we also calculate the graphs of Eq. (42) that do not contribute to the CSA, and we find

$$= -\frac{g^4}{32\pi} \left[1 - \Lambda_{\text{UV}} \left(\frac{\theta(-T)}{|\mathbf{p}_1 + \mathbf{p}_3|} + \frac{\theta(-U)}{|\mathbf{p}_1 + \mathbf{p}_4|} \right) \right]. \quad (46)$$

(Note that the S-channel graph is in fact zero, because it is made of a sequence of retarded propagators in a closed loop.) By adding Eqs. (44) and (46), we obtain the one-loop result in the unapproximated theory,

$$-i\Gamma_{1122}^{1\text{ loop}} = -\frac{g^4}{32\pi} [\theta(T) + \theta(U)], \quad (47)$$

which is ultraviolet finite, in agreement with the renormalizability of the full theory.

¹³For the graphs in Eq. (43), the integrand is of the form $\delta(K^2)\delta((P+K)^2)$ where $P \equiv p_1 + p_3$ or $P \equiv p_1 + p_4$. Using the first delta function, the argument of the second one is $(P+K)^2 = 2P \cdot K + P^2$, which is only of degree 1 in the loop momentum. Therefore, the second propagator contributes only -1 to the actual degree of divergence of the graph, contrary to the -2 assumed based on dimensionality when computing the superficial degree of divergence. This discrepancy is also related to the impossibility to perform a Wick's rotation when the integrand is expressed in terms of delta functions or retarded/advanced propagators.

D. Two-point functions at two loops

Let us also mention two problematic two-point functions at two loops. We just quote the results here (the derivation will be given in [93]), for an on-shell momentum P ($P^2 = 0, p_0 > 0$):

$$\begin{aligned}
 -i[\Sigma_{11}(P)]_{\text{CSA}}^{2 \text{ loop}} &= \text{Diagram (1)} \\
 &= -\frac{g^4}{1024\pi^3} \left(\Lambda_{\text{UV}}^2 - \frac{2}{3}p^2 \right), \tag{48}
 \end{aligned}$$

$$\begin{aligned}
 \text{Im} [\Sigma_{12}(P)]_{\text{CSA}}^{2 \text{ loop}} &= \text{Diagram (2)} \\
 &= -\frac{g^4}{1024\pi^3} \left(\Lambda_{\text{UV}}^2 - \frac{2}{3}p^2 \right). \tag{49}
 \end{aligned}$$

An ultraviolet divergence in Σ_{11} is nonrenormalizable, since there is no ϕ_1^2 operator in the Lagrangian. Similarly, the divergence at two loops in $\text{Im}\Sigma_{12}$ is also nonrenormalizable, because it would require an imaginary counterterm, that would break the Hermiticity of the Lagrangian.

V. CONSEQUENCES ON PHYSICAL OBSERVABLES

A. Order of magnitude of the pathological terms

So far, we have exhibited a four-point function at one loop that has an ultraviolet divergence in the CSA but not if computed in full, and that cannot be renormalized in the

CSA because it would require a counterterm for an operator that does not exist in the Lagrangian.

In practice, this one-loop function enters as a subdiagram in the loop expansion of observable quantities, making them unrenormalizable. In order to assess the damage, it is important to know the lowest order at which this occurs. Let us consider in this discussion two quantities that have been commonly computed with the classical statistical method: the expectation value of the energy-momentum tensor, and the occupation number, which can be extracted from the G_{22} propagator.

For the 22 component of the propagator, the first occurrence of the 1122 four-point function as a subgraph is in the following one-loop contribution:

$$[G_{22}]_{\text{CSA}}^{\text{NNLO}} = \text{Diagram (3)} \tag{50}$$

where the problematic subdiagram has been highlighted (the propagators in purple are of type G_{22}). The fact that this problematic subgraphs occurs only at one loop and beyond is related to the fact that classical statistical approximation is equivalent to the full theory up to (including) NLO. The first differences appear at NNLO, which means one loop for the G_{22} function. In a situation where the typical physical scale is denoted Q , the subdiagram is of order $g^4 \Lambda_{\text{UV}}/Q$, and the external field attached to the graph is of order $\Phi_2 \sim Q/g$ (we assume a system dominated by strong fields, as in applications to heavy ion

collisions). This one-loop contribution to G_{22} is of order $g^2 \Lambda_{\text{UV}} Q$, to be compared to Q^2/g^2 at leading order. Therefore, the relative suppression of this nonrenormalizable contribution is by a factor

$$g^4 \frac{\Lambda_{\text{UV}}}{Q}. \tag{51}$$

The same conclusion holds in the case of the energy-momentum tensor,

$$T^{\mu\nu} = (\partial^\mu \phi_2)(\partial^\nu \phi_2) - g^{\mu\nu} \left[\frac{1}{2} (\partial_\rho \phi_2)(\partial^\rho \phi_2) - \frac{m^2}{2} \phi_2^2 - \frac{g^2}{4!} \phi_2^4 \right], \quad (52)$$

for which the 1122 four-point function enters also at NNLO (in this case, this means two loops), in the following diagram:

$$[T^{\mu\nu}]_{\text{CSA}}^{\text{NNLO}} = \text{Diagram} \quad (53)$$

(The cross denotes the insertion of the $T^{\mu\nu}$ operator.) The order of magnitude of this graph is $g^2 \Lambda_{\text{UV}} Q^3$, while the leading order contribution to the energy-momentum tensor is of order Q^4/g^2 . Therefore, the relative suppression is the same as in Eq. (51).

All these examples suggest that a minimum requirement is that the ultraviolet cutoff should satisfy

$$\Lambda_{\text{UV}} \ll \frac{Q}{g^4}, \quad (54)$$

for the above contributions to give only a small contamination to their respective observables in a classical statistical computation with cutoff Λ_{UV} . However, one could be a bit more ambitious and request that this computation be also accurate at NLO. For this, we should set the cutoff so that the above diagrams are small corrections compared to the NLO contributions. This is achieved if the highlighted four-point function in these graphs is small compared to the tree-level four-point function, i.e. g^2 . This more stringent condition reads

$$\begin{aligned} \frac{g^4 \Lambda_{\text{UV}}}{16\pi Q} &\ll g^2, \\ \text{i.e. } \Lambda_{\text{UV}} &\ll \frac{16\pi Q}{g^2}, \end{aligned} \quad (55)$$

where we have reintroduced the factors 2 and π from Eq. (44), because in practical situations they are numerically important. One can see that this inequality is easy to satisfy at weak coupling $g^2 \ll 1$, and presumably only marginally satisfied at larger couplings $g \approx 1$.

B. Ultraviolet contamination at asymptotic times

The condition of Eq. (55) ensures that the pathological NNLO contributions are much smaller than the NLO corrections (the latter are correctly given by the classical statistical approximation). Another important aspect of this

discussion is whether, by ensuring that the inequality (55) is satisfied, one is guaranteed that the contamination by the pathological terms remains small at all times. It is easy to convince oneself that this is not the case. In Ref. [93], we argue that in the limit where $\Lambda_{\text{UV}} \rightarrow \infty$, these pathological terms, if not removed, induce modifications of order 1 to the particle distribution in a time of order

$$Qt_* \sim 1024\pi^3 g^{-4} (Q/\Lambda_{\text{UV}})^2. \quad (56)$$

Effectively, these ultraviolet divergent terms act as spurious scatterings¹⁴ with a rate proportional to $g^4 \Lambda_{\text{UV}}^2/Q$.

Moreover, the state reached by the system when $t \rightarrow +\infty$ is controlled solely by conservation laws and by a few quantities that characterize the initial condition, in addition to the ultraviolet cutoff. For instance, if the only conserved quantities are energy and momentum, then the asymptotic state depends only on the total energy in the system. If in addition the particle number was conserved, then the asymptotic state would also depend on the number of particles in the system.

In particular, the value of the coupling constant does not play a role in determining which state is reached at asymptotic times; it only controls how quickly the system approaches the asymptotic state. This means that, even if g^2 is small so that the inequality (55) is satisfied, the CSA may evolve the system towards an asymptotic state that differs significantly from the true asymptotic state, regardless of how small g^2 is. Therefore, the strong dependence of the asymptotic state on the ultraviolet cutoff observed in Fig. 10 of Ref. [5] is not specific to a “large” coupling $g^2 = 1$. Exactly the same cutoff dependence would be observed at smaller couplings, but the system would need to evolve for a (much) longer time in order to reach it.

C. Could it be fixed?

An important issue is whether one could somehow alter the classical statistical approximation in order to remove the linear divergence that appears in the one-loop four-point function Γ_{1122} . As a support of these considerations, let us consider the NNLO correction to the function G_{22} . Equation (50) displays the unique contribution in the classical statistical approximation. However, in the full theory there are two other possible arrangements of the internal 1/2 inside the 1122 subdiagram. This topology with the complete 1122 subdiagram reads

¹⁴This estimate can be obtained by performing the classical approximation of Ref. [80] to the Boltzmann equation with a $2 \rightarrow 2$ collision term. This classical approximation gives a spurious term in $g^4 \Lambda_{\text{UV}}^2 f(\mathbf{p})/Q$, in addition to the usual f^3 and f^2 terms. This spurious collision term stems directly from the nonrenormalizable UV divergence in the imaginary part of the self-energy Σ_{12} . If $\Lambda_{\text{UV}} \rightarrow \infty$ at fixed Q and f , this term dominates the evolution and leads to the estimate (56).

(57)

The CSA result contains only the first graph, and as a consequence it has a linear ultraviolet divergence, while the sum of the three graphs is finite. So the question is, could one reintroduce in the CSA the divergent part of the second and third graphs, in order to compensate the divergence of the first graph?

In order to better visualize what it would take to do this, let us modify the way the graphs are represented, so that they reflect the space-time evolution of the system and the *modus operandi* of practical implementations of the CSA. The modified representation for the first term in Eq. (57) is shown in Fig. 2. In this representation, the lines with arrows are retarded propagators (the time flows in the direction of the arrow). The solution of the classical equation of motion is a sum of trees made of retarded propagators, where the “leaves” of the tree are anchored to the initial surface. In the diagram shown in Fig. 2, there are two such trees, both containing one instance of the quartic interaction term.

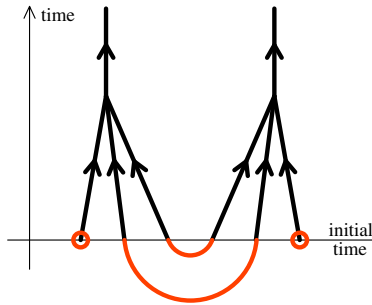


FIG. 2 (color online). Space-time representation of Eq. (50). The propagators with an arrow are retarded propagators. The orange circles represent the mean value of the initial field. The orange lines represent the link coming from the Gaussian fluctuations of the initial field.

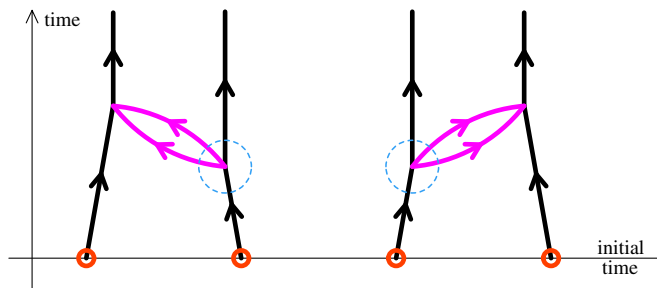


FIG. 3 (color online). Space-time representation of the NNLO contributions to G_{22} that are not included in the classical statistical approximation. The dotted circles outline the 1112 vertices, that are missing in the CSA.

order to complete the calculation in the CSA, one performs a Gaussian average over the initial value of the classical field. Diagrammatically, this average amounts to attaching the leaves of the tree to one-point objects representing the average value of the initial field, or to connecting them pairwise with the two-point function that describes the variance of the initial Gaussian distribution.

It is crucial to note that the trees that appear in the solution of the classical equation of motion are “oriented”: three retarded propagators can merge at a point, from which a new retarded propagator starts. Let us call this a $3 \rightarrow 1$ vertex (when read in the direction of increasing time). These trees do not contain any $2 \rightarrow 2$ or $1 \rightarrow 3$ vertices. Their absence is intimately related to the absence of the 1122 and 1112 vertices in the Lagrangian in the classical statistical approximation.

In Fig. 3, we now show the same representation for the second and third contributions of Eq. (57). Firstly, we see that these graphs contain a $1 \rightarrow 3$ vertex (surrounded by a dotted circle in the figure), in agreement with the fact that they do not appear in the CSA. There is no way to generate the loop contained in these graphs via the average over the initial conditions, because this loop corresponds to quantum fluctuations that happen later on in the time evolution. By Fourier transforming the divergent part of these diagrams in Eq. (46), we can readily see that it is proportional to

$$\frac{1}{|\mathbf{x} - \mathbf{y}|} \delta((x^0 - y^0)^2 - (\mathbf{x} - \mathbf{y})^2) \quad (58)$$

in coordinate space. Thus, the divergent part of these loops is nonlocal, with support on the light cone, as illustrated in Fig. 4.

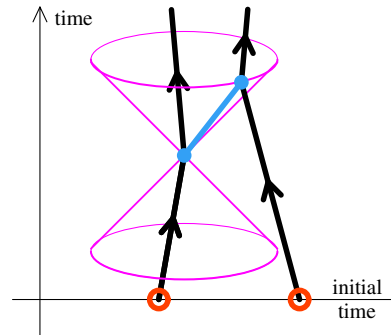


FIG. 4 (color online). Space-time representation of the divergent part of the graphs of Fig. 3. As explained in the text, these divergent terms are nonlocal in space-time, with support on the light cone.

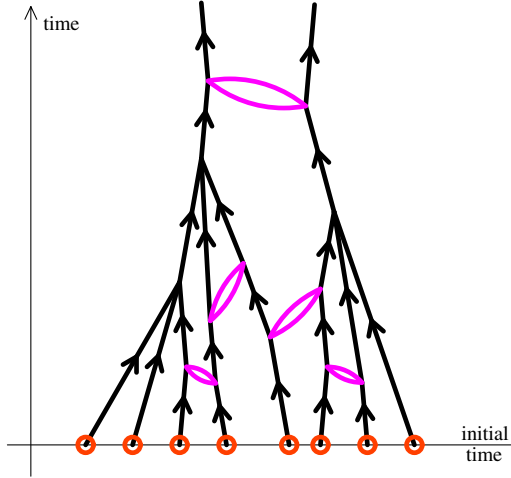


FIG. 5 (color online). Contribution to G_{22} with many Γ_{1122} subgraphs.

There can also be arbitrarily many occurrences of these divergent subgraphs in the calculation of an observable in the classical statistical method, as illustrated in Fig. 5 in the case of G_{22} . This implies that these divergences cannot be removed by an overall subtraction, and that one must instead modify the Lagrangian. One could formally subtract them by adding to the action of the theory a nonlocal counterterm¹⁵ of the form

$$\Delta S \equiv -\frac{i}{2} \int d^4x d^4y [\phi_1(x) \phi_2(x)] v(x, y) [\phi_1(y) \phi_2(y)], \quad (59)$$

where we define¹⁶

$$v(x, y) \equiv \frac{g^4}{64\pi^3} \frac{\Lambda_{UV}}{|\mathbf{x} - \mathbf{y}|} \delta((x^0 - y^0)^2 - (\mathbf{x} - \mathbf{y})^2). \quad (60)$$

In order to deal with such a term, the simplest is to perform a *Hubbard-Stratonovich* transformation [94,95], by introducing an auxiliary field $\zeta(x)$ via the following identity:

$$e^{i\Delta S} = \int [D\zeta] e^{\frac{i}{2} \int_{x,y} \zeta(x) v^{-1}(x,y) \zeta(y)} e^{i \int_x \zeta(x) \phi_1(x) \phi_2(x)}. \quad (61)$$

¹⁵Of course, there was no $\phi_1^2 \phi_2^2$ term in the original bare action. On the other hand, we know that in the full theory, there should not be an intrinsic ultraviolet divergence in the 1122 function. One should view this counterterm as a way of reintroducing some of the terms that are beyond the classical statistical approximation, in order to restore the finiteness of the 1122 function.

¹⁶The definition (59) is a *minimal subtraction* where only terms proportional to the ultraviolet cutoff are included. It is possible to add a finite part to the function $v(x, y)$,

$$v_{\text{finite}}(x, y) \equiv -\frac{g^4}{32\pi} \delta(x - y),$$

in order to recover the complete one-loop result for the function Γ_{1122} .

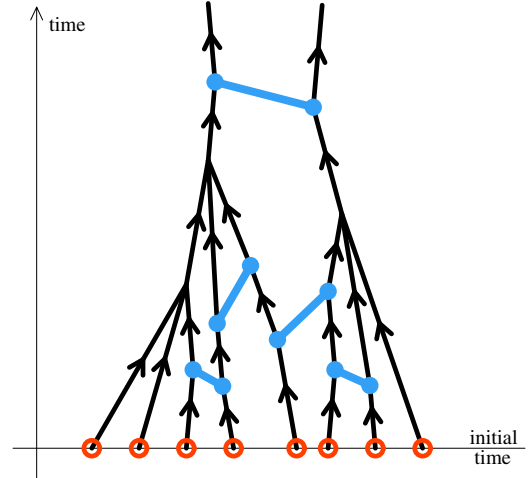


FIG. 6 (color online). Effect of the noise term on the topology shown in Fig. 5.

The advantage of this transformation is that we have transformed a nonlocal four-field interaction term into a local interaction with a random Gaussian auxiliary field.

The rest of the derivation of the classical statistical method remains the same: the field ϕ_1 appears as a Lagrange multiplier for a classical equation of motion for the field φ , but now we get an extra, stochastic, term in this equation:

$$(\square + m^2)\varphi + \frac{g^2}{6}\varphi^3 + i\xi\varphi = j. \quad (62)$$

Note that we have introduced $\zeta \equiv i\xi$ in order to have a positive definite variance for the new variable ξ . From the above derivation, this noise must be Gaussian distributed, with a mean and variance given by the following formulas:

$$\begin{aligned} \langle \xi(x) \rangle &= 0 \\ \langle \xi(x) \xi(y) \rangle &= \frac{g^4}{64\pi^3} \frac{\Lambda_{UV}}{|\mathbf{x} - \mathbf{y}|} \delta((x^0 - y^0)^2 - (\mathbf{x} - \mathbf{y})^2). \end{aligned} \quad (63)$$

By construction, the noise term in Eq. (62), once averaged with Eq. (63), will insert a nonlocal counterterm in every place where the Γ_{1122} function can appear. For instance, when applied to the calculation of G_{22} , the contribution shown in Fig. 5 will be accompanied by the term shown in Fig. 6.

Although the noise in Eq. (63) has nonlocal space-time correlations, it is easy to generate it in momentum space, where it becomes diagonal. The main practical difficulty however comes from the nonlocality in time¹⁷: one would

¹⁷This nonlocality appears to be a reminiscence of the memory effects that exist in the full quantum field theory, but are discarded in the classical statistical approximation. Such a nonlocality in time is also present in the 2PI resummation scheme, which is known to be renormalizable [41,42,96–98].

need to generate and store the whole spatiotemporal dependence for each configuration of the noise term prior to solving the modified classical equation of motion.

The noise term introduced in Eq. (62) is purely imaginary, and it turns the classical field ϕ into a complex valued quantity. However, since ξ is Gaussian distributed with a zero mean, any Hermitian observable constructed from ϕ via an average over ξ will be real valued.¹⁸ Equation (62) is therefore a complex Langevin equation, and may be subject to the problems encountered with this kind of equation (lack of convergence, or convergence to the incorrect solution; see Refs. [99–104] and references therein for recent discussions of these issues). At the moment, it is an open question whether Eq. (62) really offers a practical way of removing the linear ultraviolet divergences from the classical statistical approximation.

VI. CONCLUSIONS AND OUTLOOK

In this work, we have investigated the ultraviolet behavior of the classical statistical approximation, used to evaluate expectation values of observables in a system of scalar fields initialized in the vacuum state and driven out of equilibrium by a strong external source. This has been done by using perturbation theory in the retarded-advanced basis, where this approximation has a very simple expression, and in calculating all the one-loop subdiagrams that can possibly be generated with these diagrammatic rules.

The main conclusion of this study is that the classical approximation leads to a one-loop four-point function that diverges linearly in the ultraviolet cutoff. More specifically, the problem lies in the function Γ_{1222} , where the 1,2 indices refer to the retarded-advanced basis. In the unapproximated theory, this function is ultraviolet finite, but it violates Weinberg’s theorem in the classical statistical approximation, because it has an ultraviolet divergence with a coefficient which is nonpolynomial in the external momenta. Moreover, it is nonrenormalizable because it corresponds to an operator that does not even appear in the Lagrangian one started from.

The mere existence of these divergent terms implies that the classical statistical approximation is not renormalizable, no matter what the value of the coupling constant is.

We have estimated that the contamination of the results by these nonrenormalizable terms is of relative order $g^4 \Lambda_{UV}/Q$, where Q is the typical physical momentum scale of the problem under consideration. Based on this, the general rule is that the coupling should not be too large, and the cutoff should remain close enough to the physical scales.

In this paper, we have also proposed that this one-loop spurious (because it does not exist in the full theory) divergence may be subtracted by adding a multiplicative Gaussian noise term to the classical equation of motion. This noise term can be tuned in order to reintroduce some of the terms of the full theory that had been lost when doing the classical approximation. In order to subtract the appropriate quantity, this noise must be purely imaginary, with a two-point correlation given by the Fourier transform of the divergent term. Unfortunately, this correlation is nonlocal in time, which makes the implementation of this correction quite complicated. Whether this can be done in practice remains an open question at this point.

Moreover, the ultraviolet contamination due to these nonrenormalizable terms is cumulative over time, and will eventually dominate the dynamics of the system no matter how small $g^4 \Lambda_{UV}/Q$ is. This can be easily understood in the quasiparticle approximation [80,105], in which the quadratic UV divergences of the self-energies (48) and (49) appear in the collision term in the corresponding Boltzmann equation. An extensive discussion of this asymptotic ultraviolet sensitivity, and of the time evolution that leads to the asymptotic state, will be provided in a forthcoming work [93].

ACKNOWLEDGMENTS

We would like to thank L. McLerran for useful discussions about this work and closely related issues. This work is supported by the Agence Nationale de la Recherche project 11-BS04-015-01.

APPENDIX A: Γ_{1222} AND Γ_{1112} AT ONE LOOP

At one loop, the four-point functions Γ_{1222} and Γ_{1112} are given by the following sets of graphs:

$$\begin{aligned}
 -i\Gamma_{1222}^{\text{1 loop}}(p_1 \cdots p_4) &= \text{Diagram 1} + \text{Diagram 2} + \text{Diagram 3} \\
 &= -i [I(p_3 + p_4) + I(p_2 + p_3) + I(p_2 + p_4)] , \tag{A1}
 \end{aligned}$$

¹⁸The average over ξ will only retain terms that are even in ξ , and the factors i will cancel.

$$\begin{aligned}
 -i\Gamma_{2111}^{1 \text{ loop}}(p_1 \cdots p_4) &= \text{Diagram 1} + \text{Diagram 2} + \text{Diagram 3} \\
 &= -\frac{i}{4} [I(p_3 + p_4) + I(p_2 + p_3) + I(p_2 + p_4)] .
 \end{aligned} \tag{A2}$$

Note that all the one-loop contributions to Γ_{1112} are zero if we exclude the 1112 vertex, as done in the classical statistical approximation. The fact that Γ_{1222} and Γ_{2111} differ only by a factor 1/4 is a consequence of their common origin in the Schwinger-Keldysh formalism, where the $+++$ and $---$ vertex functions are mutual complex conjugates.

They are all expressible in terms of a single loop integral,

$$I(P) \equiv -ig^4 \int \frac{d^4 K}{(2\pi)^4} G_{22}(K) G_{12}(P + K). \tag{A3}$$

Since $G_{22}(K)$ is a delta function $\delta(K^2)$, we use it in order to perform the integration over the energy k^0 . Then, the integration over $\cos(\theta)$, where θ is the angle between the three-vectors \mathbf{p} and \mathbf{k} , is elementary but requires that one studies carefully whether $P^2 + 2\mathbf{P} \cdot \mathbf{K}$ can vanish in the integration range. If this quantity can vanish, the integral will also have an imaginary part. This leads to the following expression for $I(P)$:

$$\begin{aligned}
 I(P) &= \frac{g^4}{32\pi^2} \left\{ \frac{1}{p} \int_0^{\Lambda_{UV}} dk \sum_{\epsilon=\pm 1} \log \left| \frac{p + \epsilon p^0 + P^2/2k}{p - \epsilon p^0 - P^2/2k} \right| + i\pi \left(\theta(P^2) \text{sign}(p^0) - \theta(-P^2) \frac{p^0}{p} \right) \right\} \\
 &= \frac{g^4}{32\pi^2} \left\{ \ln \left| \frac{P^2}{4\Lambda_{UV}^2} \right| + \frac{p^0}{p} \log \left| \frac{p^0 + p}{p^0 - p} \right| - 2 + i\pi \left(\theta(P^2) \text{sign}(p^0) - \theta(-P^2) \frac{p^0}{p} \right) \right\}.
 \end{aligned} \tag{A4}$$

Therefore, the real part is logarithmically ultraviolet divergent, while the imaginary part is finite.

APPENDIX B: Γ_{1122} AT ONE LOOP

In this appendix, we perform the calculation of some of the graphs contributing to $\Gamma_{1122}^{1 \text{ loop}}$. The list of all the relevant graphs is given in Eq. (42). The unique S-channel graph is zero, because it has a closed loop of retarded propagators. Since the T- and U-channel graphs are identical, up to the permutation $p_3 \leftrightarrow p_4$, we will calculate only the T-channel graphs here.

1. Classical statistical approximation at one loop

Let us consider first the graph that contributes in the classical statistical approximation:

$$\text{Diagram 4} = -\frac{g^4}{2} \int \frac{d^4 K}{(2\pi)^4} \pi \delta(K^2) \pi \delta((P - K)^2), \tag{B1}$$

where we denote $P \equiv p_1 + p_3$. We first use the $\delta(K^2)$ in order to perform the integral over k^0 , which gives

$$\text{Diagram 4} = -\frac{g^4}{32\pi} \int_0^{\Lambda_{UV}} k dk \int_{-1}^{+1} d(\cos \theta) \sum_{\epsilon=\pm} \delta(P^2 - 2\epsilon k p^0 + 2pk \cos \theta), \tag{B2}$$

Anticipating the fact that the integral over $k = |\mathbf{k}|$ is ultraviolet divergent, we have introduced an upper cutoff on this integral. The second step is to use the remaining delta function in order to integrate over $\cos \theta$. This requires some careful analysis, in order to determine whether there is a valid solution, i.e. one for which $-1 \leq \cos \theta \leq +1$. This depends on the sign ϵ , on the sign of P^2 and on the value of k . The results are summarized here:

(1) If $P^2 > 0$, there is a valid solution if and only if

$$\epsilon p^0 > 0 \quad \text{and} \quad \frac{|p^0| - p}{2} \leq k \leq \frac{|p^0| + p}{2},$$

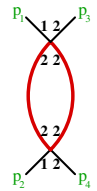
(2) If $P^2 < 0$,

(a) There is no solution if $k < \frac{p - |p^0|}{2}$

(b) If $\epsilon p^0 < 0$, there is a solution if $\frac{p - |p^0|}{2} \leq k$

(c) If $\epsilon p^0 > 0$, there is a solution if $\frac{p + |p^0|}{2} \leq k$

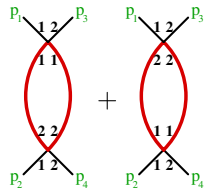
Using this, the integration over $\cos \theta$ leads to a piecewise constant integrand for the remaining integral. We eventually obtain



$$= -\frac{g^4}{64\pi} \left[\text{sign}(P^2) + 2 \Lambda_{\text{UV}} \frac{\theta(-P^2)}{|P|} \right]. \quad (\text{B3})$$

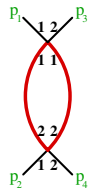
2. One-loop graphs beyond the CSA

Let us now focus on the second and third T-channel graphs,



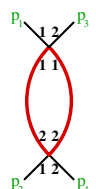
$$= -\frac{g^4}{8} \int \frac{d^4 K}{(2\pi)^4} [G_R(K)G_R(P-K) + G_A(K)G_A(P-K)]. \quad (\text{B4})$$

Changing $K^\mu \rightarrow -K^\mu$ in the second term, we see that this term is the same as the first one with the change $P^\mu \rightarrow -P^\mu$. Therefore, we need only to calculate the first term, multiply by two its P -even part and discard its P -odd part. The first step is to perform the k^0 integral in the complex plane. By closing the integration contour in the lowest half-plane, we pick the two poles of $G_R(K)$, and we get



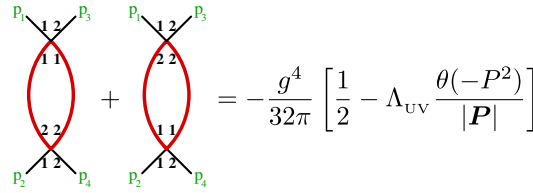
$$= -\frac{g^4}{64\pi^2} \int_0^{\Lambda_{\text{UV}}} k dk \int_{-1}^{+1} d(\cos \theta) \sum_{\epsilon=\pm} \epsilon [G_R(P-K)]_{k^0=\epsilon k}. \quad (\text{B5})$$

At this point, one can decompose the retarded propagator into a principal value term and a delta function. One can check that the principal value gives only terms that are P odd, that we can thus drop. Keeping only the delta function leads to



$$= -\frac{g^4}{64\pi} \int_0^{\Lambda_{\text{UV}}} k dk \int_{-1}^{+1} d(\cos \theta) \sum_{\epsilon=\pm} \text{sign}(\epsilon p^0 - k) \delta(P^2 - 2\epsilon k p^0 + 2pk \cos \theta). \quad (\text{B6})$$

We proceed by using the delta function to perform the integral over $\cos \theta$. The conditions for having a valid solution are the same as before. Finally, we obtain

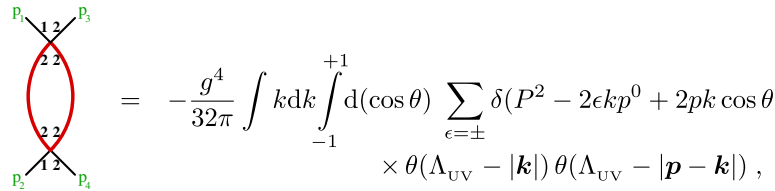


$$\begin{aligned}
 & \text{Diagram 1} + \text{Diagram 2} = -\frac{g^4}{32\pi} \left[\frac{1}{2} - \Lambda_{\text{UV}} \frac{\theta(-P^2)}{|\mathbf{P}|} \right] \quad (\text{B7})
 \end{aligned}$$

3. CSA result with symmetric regularization

The ultraviolet regularization introduced in Eq. (B2) is not entirely satisfactory, because it breaks the symmetry between the two internal lines of the graph, by placing a cutoff Λ_{UV} on the 3-momentum $|\mathbf{k}|$, while the 3-momentum $|\mathbf{p} - \mathbf{k}|$ in the other internal line is not constrained.

It is perfectly fine to do so. However, some important identities obeyed by two-loop self-energies, in which the one-loop Γ_{1122} function appears as a subgraph, rely on the symmetry between the internal lines of the graph. It is therefore important that the regularization scheme employed in intermediate steps of the calculation does not break this symmetry, and in particular that the subgraph itself respects this symmetry. This issue will be discussed at length in a forthcoming work, Ref. [93], but for later reference we present here the formulas for the function Γ_{1122} at one loop with a symmetric regularization. This just amounts to replacing Eq. (B2) by



$$\begin{aligned}
 & \text{Diagram} = -\frac{g^4}{32\pi} \int k dk \int_{-1}^{+1} d(\cos \theta) \sum_{\epsilon=\pm} \delta(P^2 - 2\epsilon k p^0 + 2pk \cos \theta) \\
 & \quad \times \theta(\Lambda_{\text{UV}} - |\mathbf{k}|) \theta(\Lambda_{\text{UV}} - |\mathbf{p} - \mathbf{k}|), \quad (\text{B8})
 \end{aligned}$$

with $|\mathbf{p} - \mathbf{k}| = (p^2 + k^2 - 2pk \cos \theta)^{1/2}$. The new constraint on $|\mathbf{p} - \mathbf{k}|$ slightly complicates the discussion of the various cases, and in the end we obtain

$$-\frac{g^4}{32\pi p} \times \begin{cases} \left[\Lambda_{\text{UV}} - \frac{p+|p_0|}{2} \right] \theta \left(\Lambda_{\text{UV}} - \frac{p+|p_0|}{2} \right) & [P^2 < 0] \\ \frac{p}{2} & \left[P^2 > 0, \frac{p+|p_0|}{2} \leq \Lambda_{\text{UV}} \right] \\ \Lambda_{\text{UV}} - \frac{|p_0|}{2} & \left[P^2 > 0, \frac{|p_0|}{2} \leq \Lambda_{\text{UV}} \leq \frac{p+|p_0|}{2} \right] \\ 0 & \left[P^2 > 0, \Lambda_{\text{UV}} \leq \frac{|p_0|}{2} \right] \end{cases} \quad (\text{B9})$$

instead of Eq. (B3). Note that the ultraviolet divergence itself (i.e. the terms that diverge when $\Lambda_{\text{UV}} \rightarrow +\infty$ at fixed P^μ) is not affected by this modification of the regularization procedure.

- [1] J. Berges, J. P. Blaizot, and F. Gelis, *J. Phys. G* **39**, 085115 (2012).
- [2] J. Berges, K. Boguslavski, and S. Schlichting, *Phys. Rev. D* **85**, 076005 (2012).
- [3] J. Berges, K. Boguslavski, S. Schlichting, and R. Venugopalan, *Phys. Rev. D* **89**, 074011 (2014).
- [4] J. Berges, K. Boguslavski, S. Schlichting, and R. Venugopalan, *Phys. Rev. D* **89**, 114007 (2014).
- [5] J. Berges, K. Boguslavski, S. Schlichting, and R. Venugopalan, *J. High Energy Phys.* 05 (2014) 054.
- [6] J. Berges, D. Gelfand, S. Scheffler, and D. Sexty, *Phys. Lett. B* **677**, 210 (2009).
- [7] J. Berges and D. Sexty, *Phys. Rev. Lett.* **108**, 161601 (2012).
- [8] J. Berges, S. Schlichting, and D. Sexty, *Phys. Rev. D* **86**, 074006 (2012).
- [9] K. Fukushima and F. Gelis, *Nucl. Phys.* **A874**, 108 (2012).
- [10] K. Fukushima, *Phys. Rev. C* **89**, 024907 (2014).
- [11] T. Kunihiro, B. Muller, A. Ohnishi, A. Schafer, T. T. Takahashi, and A. Yamamoto, *Phys. Rev. D* **82**, 114015 (2010).
- [12] H. Iida, T. Kunihiro, B. Mueller, A. Ohnishi, A. Schafer, and T. T. Takahashi, *Phys. Rev. D* **88**, 094006 (2013).
- [13] K. Dusling, T. Epelbaum, F. Gelis, and R. Venugopalan, *Nucl. Phys.* **A850**, 69 (2011).
- [14] T. Epelbaum and F. Gelis, *Nucl. Phys.* **A872**, 210 (2011).
- [15] K. Dusling, T. Epelbaum, F. Gelis, and R. Venugopalan, *Phys. Rev. D* **86**, 085040 (2012).
- [16] T. Epelbaum and F. Gelis, *Phys. Rev. D* **88**, 085015 (2013).
- [17] T. Epelbaum and F. Gelis, *Phys. Rev. Lett.* **111**, 232301 (2013).
- [18] A. Kurkela and G. D. Moore, *J. High Energy Phys.* 12 (2011) 044.
- [19] A. Kurkela and G. D. Moore, *J. High Energy Phys.* 11 (2011) 120.
- [20] A. Kurkela and G. D. Moore, *Phys. Rev. D* **86**, 056008 (2012).
- [21] M. C. Abreu, A. Kurkela, E. Lu, and G. D. Moore, *Phys. Rev. D* **89**, 074036 (2014).
- [22] M. Attems, A. Rebhan, and M. Strickland, *Phys. Rev. D* **87**, 025010 (2013).
- [23] J. P. Blaizot, F. Gelis, J. Liao, L. McLerran, and R. Venugopalan, *Nucl. Phys.* **A873**, 68 (2012).
- [24] J. P. Blaizot, J. Liao, and L. D. McLerran, *Nucl. Phys.* **A920**, 58 (2013).
- [25] M. P. Heller, R. A. Janik, and P. Witaszczyk, *Phys. Rev. Lett.* **108**, 201602 (2012).
- [26] J. Casalderrey-Solana, M. P. Heller, D. Mateos, and W. van der Schee, *Phys. Rev. Lett.* **111**, 181601 (2013).
- [27] B. Wu, *J. High Energy Phys.* 04 (2013) 044.
- [28] U. Reinosa and J. Serreau, *Ann. Phys. (Amsterdam)* **325**, 969 (2010).
- [29] F. Gautier and J. Serreau, *Phys. Rev. D* **86**, 125002 (2012).
- [30] A. Giraud and J. Serreau, *Phys. Rev. Lett.* **104**, 230405 (2010).
- [31] S. Floerchinger and C. Wetterich, *J. High Energy Phys.* 03 (2014) 121.
- [32] T. Gasenzer and J. M. Pawłowski, *Phys. Lett. B* **670**, 135 (2008).
- [33] T. Gasenzer, S. Kessler, and J. M. Pawłowski, *Eur. Phys. J. C* **70**, 423 (2010).
- [34] P. Arnold, G. D. Moore, and L. G. Yaffe, *J. High Energy Phys.* 01 (2003) 030.
- [35] J. M. Luttinger and J. C. Ward, *Phys. Rev.* **118**, 1417 (1960).
- [36] G. Baym and L. P. Kadanoff, *Phys. Rev.* **124**, 287 (1961).
- [37] C. de Dominicis and P. C. Martin, *J. Math. Phys. (N.Y.)* **5**, 14 (1964).
- [38] C. de Dominicis and P. C. Martin, *J. Math. Phys. (N.Y.)* **5**, 31 (1964).
- [39] J. M. Cornwall, R. Jackiw, and E. Tomboulis, *Phys. Rev. D* **10**, 2428 (1974).
- [40] J. Berges, *AIP Conf. Proc.* **739**, 3 (2005).
- [41] J. Berges, S. Borsányi, U. Reinosa, and J. Serreau, *Ann. Phys. (Amsterdam)* **320**, 344 (2005).
- [42] U. Reinosa and J. Serreau, *J. High Energy Phys.* 07 (2006) 028.
- [43] A. Branschadel and T. Gasenzer, *J. Phys. B* **41**, 135302 (2008).
- [44] G. Aarts, N. Laurie, and A. Tranberg, *Phys. Rev. D* **78**, 125028 (2008).
- [45] Y. Hatta and A. Nishiyama, *Nucl. Phys.* **A873**, 47 (2012).
- [46] Y. Hatta and A. Nishiyama, *Phys. Rev. D* **86**, 076002 (2012).
- [47] E. Iancu, A. Leonidov, and L. D. McLerran, “Lectures given at Cargese Summer School on QCD Perspectives on Hot and Dense Matter,” 2001.
- [48] E. Iancu and R. Venugopalan, *Quark Gluon Plasma 3*, edited by R. C. Hwa and X. N. Wang (World Scientific, Singapore), 2004.
- [49] T. Lappi and L. D. McLerran, *Nucl. Phys.* **A772**, 200 (2006).
- [50] F. Gelis, E. Iancu, J. Jalilian-Marian, and R. Venugopalan, *Annu. Rev. Nucl. Part. Sci.* **60**, 463 (2010).
- [51] F. Gelis, *Int. J. Mod. Phys. A* **28**, 1330001 (2013).
- [52] D. Polarski and A. A. Starobinsky, *Classical Quantum Gravity* **13**, 377 (1996).
- [53] D. T. Son, [arXiv:hep-ph/9601377](https://arxiv.org/abs/hep-ph/9601377).
- [54] S. Yu. Khlebnikov and I. I. Tkachev, *Phys. Rev. Lett.* **77**, 219 (1996).
- [55] F. Gelis, T. Lappi, and R. Venugopalan, *Int. J. Mod. Phys. E* **16**, 2595 (2007).
- [56] K. Fukushima, F. Gelis, and L. McLerran, *Nucl. Phys.* **A786**, 107 (2007).
- [57] S. Jeon, *Ann. Phys. (Amsterdam)* **340**, 119 (2014).
- [58] D. Bodeker, L. D. McLerran, and A. Smilga, *Phys. Rev. D* **52**, 4675 (1995).
- [59] P. Arnold, D. T. Son, and L. G. Yaffe, *Phys. Rev. D* **55**, 6264 (1997).
- [60] G. Aarts and J. Smit, *Phys. Lett. B* **393**, 395 (1997).
- [61] G. Aarts and J. Smit, *Nucl. Phys.* **B511**, 451 (1998).
- [62] G. Aarts, B. J. Nauta, and C. G. van Weert, *Phys. Rev. D* **61**, 105002 (2000).
- [63] D. Y. Grigoriev and V. A. Rubakov, *Nucl. Phys.* **B299**, 67 (1988).
- [64] D. Y. Grigoriev, V. A. Rubakov, and M. E. Shaposhnikov, *Nucl. Phys.* **B326**, 737 (1989).
- [65] D. Y. Grigoriev, V. A. Rubakov, and M. E. Shaposhnikov, *Phys. Lett. B* **216**, 172 (1989).

- [66] J. Ambjorn, M. Laursen, and M. E. Shaposhnikov, *Phys. Lett. B* **197**, 49 (1987).
- [67] J. Ambjorn, M. Laursen, and M. E. Shaposhnikov, *Nucl. Phys.* **B316**, 483 (1989).
- [68] J. Ambjorn, T. Askgaard, H. Porter, and M. E. Shaposhnikov, *Phys. Lett. B* **244**, 479 (1990).
- [69] J. Ambjorn, T. Askgaard, H. Porter, and M. E. Shaposhnikov, *Nucl. Phys.* **B353**, 346 (1991).
- [70] J. Ambjorn and K. Farakos, *Phys. Lett. B* **294**, 248 (1992).
- [71] J. Schwinger, *J. Math. Phys. (N.Y.)* **2**, 407 (1961).
- [72] L. V. Keldysh, *Sov. Phys. JETP* **20**, 1018 (1964).
- [73] P. Aurenche and T. Becherawy, *Nucl. Phys.* **B379**, 259 (1992).
- [74] M. A. van Eijck, R. Kobes, and Ch. G. van Weert, *Phys. Rev. D* **50**, 4097 (1994).
- [75] F. Gelis, *Nucl. Phys.* **B508**, 483 (1997).
- [76] F. Gelis and R. Venugopalan, *Nucl. Phys.* **A776**, 135 (2006).
- [77] F. Gelis, T. Lappi, and R. Venugopalan, *Phys. Rev. D* **78**, 054019 (2008).
- [78] F. Gelis, T. Lappi, and R. Venugopalan, *Phys. Rev. D* **78**, 054020 (2008).
- [79] G. Aarts and J. Berges, *Phys. Rev. Lett.* **88**, 041603 (2002).
- [80] S. Jeon, *Phys. Rev. C* **72**, 014907 (2005).
- [81] A. Arrizabalaga, J. Smit, and A. Tranberg, *J. High Energy Phys.* **10** (2004) 017.
- [82] G. D. Moore, *J. High Energy Phys.* **11** (2001) 021.
- [83] A. Tranberg and B. Wu, *J. High Energy Phys.* **07** (2012) 087.
- [84] F. J. Dyson, *Phys. Rev.* **75**, 1736 (1949).
- [85] S. Weinberg, *Phys. Rev.* **118**, 838 (1960).
- [86] Y. Hahn and W. Zimmermann, *Commun. Math. Phys.* **10**, 330 (1968).
- [87] W. Zimmermann, *Commun. Math. Phys.* **11**, 1 (1968).
- [88] W. E. Caswell and A. D. Kennedy, *Phys. Rev. D* **25**, 392 (1982).
- [89] W. E. Caswell and A. D. Kennedy, *Phys. Rev. D* **28**, 3073 (1983).
- [90] J. C. Collins, *Renormalization* (Cambridge University Press, Cambridge, England, 1984).
- [91] R. E. Cutkosky, *J. Math. Phys. (N.Y.)* **1**, 429 (1960).
- [92] G. 't Hooft and M. J. G. Veltman, CERN Report No. 73-9.
- [93] T. Epelbaum, F. Gelis, N. Tanji, and B. Wu, [arXiv:1409.0701](https://arxiv.org/abs/1409.0701).
- [94] J. Hubbard, *Phys. Rev. Lett.* **3**, 77 (1959).
- [95] R. L. Stratonovich, *Sov. Phys. Dokl.* **2**, 416 (1957).
- [96] A. Arrizabalaga and U. Reinosa, *Nucl. Phys.* **A785**, 234 (2007).
- [97] Sz. Borsanyi and U. Reinosa, *Phys. Rev. D* **80**, 125029 (2009).
- [98] M. Garny and M. M. Muller, *Phys. Rev. D* **80**, 085011 (2009).
- [99] A. Mollgaard and K. Splittorff, *Phys. Rev. D* **88**, 116007 (2013).
- [100] D. Sexty, [arXiv:1310.6186](https://arxiv.org/abs/1310.6186).
- [101] J. Greensite, [arXiv:1406.4558](https://arxiv.org/abs/1406.4558).
- [102] G. Aarts, L. Bongiovanni, E. Seiler, D. Sexty, and I. O. Stamatescu, [arXiv:1310.7412](https://arxiv.org/abs/1310.7412).
- [103] L. Bongiovanni, G. Aarts, E. Seiler, D. Sexty, and I. O. Stamatescu, [arXiv:1311.1056](https://arxiv.org/abs/1311.1056).
- [104] G. Aarts, L. Bongiovanni, E. Seiler, and D. Sexty, [arXiv:1407.2090](https://arxiv.org/abs/1407.2090).
- [105] A. H. Mueller and D. T. Son, *Phys. Lett. B* **582**, 279 (2004).